

## PDF hosted at the Radboud Repository of the Radboud University Nijmegen

The following full text is a publisher's version.

For additional information about this publication click this link.

<http://hdl.handle.net/2066/81786>

Please be advised that this information was generated on 2021-09-21 and may be subject to change.

## Parathyroid Hormone Activates TRPV5 via PKA-Dependent Phosphorylation

Theun de Groot,\* Kyupil Lee,\* Michiel Langeslag,<sup>†</sup> Qi Xi,\* Kees Jalink,<sup>†</sup> René J.M. Bindels,\* and Joost G.J. Hoenderop\*

\*Department of Physiology, Radboud University Nijmegen Medical Centre, Nijmegen, and <sup>†</sup>Department of Cell Biology, Netherlands Cancer Institute, Amsterdam, Netherlands

### ABSTRACT

Low extracellular calcium ( $\text{Ca}^{2+}$ ) promotes release of parathyroid hormone (PTH), which acts on multiple organs to maintain overall  $\text{Ca}^{2+}$  balance. In the distal part of the nephron, PTH stimulates active  $\text{Ca}^{2+}$  reabsorption via the adenylyl cyclase–cAMP–protein kinase A (PKA) pathway, but the molecular target of this pathway is unknown. The transient receptor potential vanilloid 5 (TRPV5) channel constitutes the luminal gate for  $\text{Ca}^{2+}$  entry in the distal convoluted tubule and has several putative PKA phosphorylation sites. Here, we investigated the effect of PTH-induced cAMP signaling on TRPV5 activity. Using fluorescence resonance energy transfer, we studied cAMP and  $\text{Ca}^{2+}$  dynamics during PTH stimulation of HEK293 cells that coexpressed the PTH receptor and TRPV5. PTH increased cAMP levels, followed by a rise in TRPV5-mediated  $\text{Ca}^{2+}$  influx. PTH (1 to 31) and forskolin, which activate the cAMP pathway, mimicked the stimulation of TRPV5 activity. Remarkably, TRPV5 activation was limited to conditions of strong intracellular  $\text{Ca}^{2+}$  buffering. Cell surface biotinylation studies demonstrated that forskolin did not affect TRPV5 expression on the cell surface, suggesting that it alters the single-channel activity of a fixed number of TRPV5 channels. Application of the PKA catalytic subunit, which phosphorylated TRPV5, directly increased TRPV5 channel open probability. Alanine substitution of threonine-709 abolished both *in vitro* phosphorylation and PTH-mediated stimulation of TRPV5. In summary, PTH activates the cAMP-PKA signaling cascade, which rapidly phosphorylates threonine-709 of TRPV5, increasing the channel's open probability and promoting  $\text{Ca}^{2+}$  reabsorption in the distal nephron.

*J Am Soc Nephrol* 20: 1693–1704, 2009. doi: 10.1681/ASN.2008080873

Calcium ( $\text{Ca}^{2+}$ ) is essential for numerous physiologic functions and many cellular processes, including signal transduction, cell motility, and morphology.<sup>1,2</sup> The body maintains extracellular  $\text{Ca}^{2+}$  levels within a narrow range. Slight perturbations in  $\text{Ca}^{2+}$  homeostasis are detected by the  $\text{Ca}^{2+}$ -sensing receptor, located in the parathyroid glands.<sup>3</sup> Low extracellular  $\text{Ca}^{2+}$  levels inhibit  $\text{Ca}^{2+}$ -sensing receptor activity, causing the release of parathyroid hormone (PTH) into the circulation.<sup>3,4</sup> In the kidney, PTH reduces  $\text{Ca}^{2+}$  excretion by stimulating  $\text{Ca}^{2+}$  reabsorption from the distal part of the nephron.<sup>5</sup> Secreted PTH consists of 84 amino acids. Upon binding to the PTH receptor (PTH1R), it is able to activate both protein kinase C (PKC), via phospholipase C (PLC), and adenylyl cyclase-

cAMP, depending on the cell type.<sup>6,7</sup> Activation of the latter pathway requires the first two residues within the amino-terminus of PTH. Consequently, PTH (3 to 34) does not affect basal cAMP levels in contrast to PTH (1 to 34).<sup>8–10</sup> Use of full-length PTH and these fragments has implicated both path-

Received August 20, 2008. Accepted March 9, 2009.

Published online ahead of print. Publication date available at www.jasn.org.

T.d.G. and K.L. contributed equally to this work.

**Correspondence:** Dr. Joost Hoenderop, 286 Physiology, Radboud University Nijmegen Medical Centre, P.O. Box 9101, 6500 HB Nijmegen, Netherlands. Phone: +31-24-3610580; Fax: +31-24-3616413; E-mail: j.hoenderop@ncmls.ru.nl

Copyright © 2009 by the American Society of Nephrology

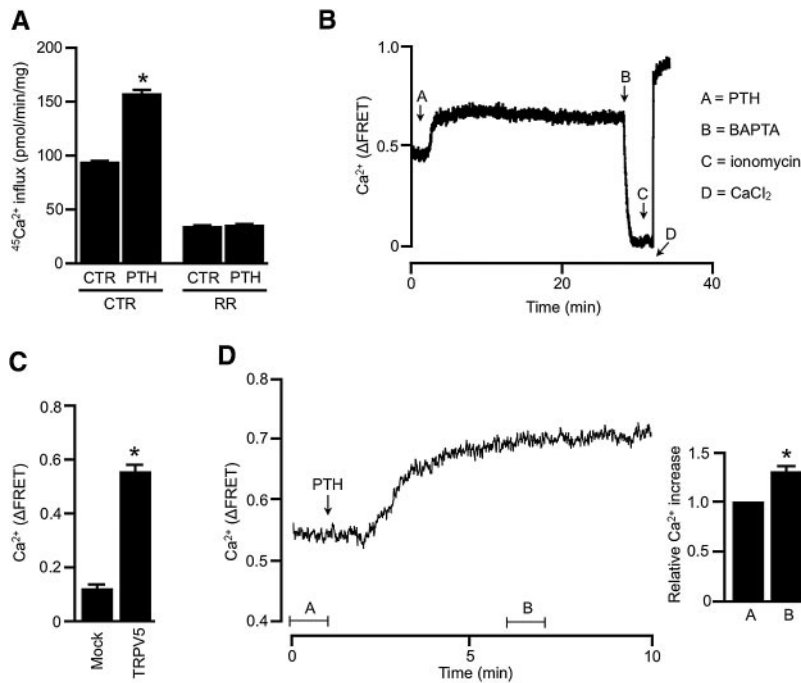


**Figure 1.** PTH rapidly induces a sustained stimulation of TRPV5-mediated  $\text{Ca}^{2+}$  influx in HEK293 cells transiently coexpressing PTH1R and TRPV5, pretreated for 30 min with 25  $\mu\text{M}$  BAPTA-AM. All procedures were performed at 37°C, and PTH or DMSO solvent (CTR) was administered simultaneously with  $^{45}\text{Ca}^{2+}$ . \* $P < 0.05$  versus CTR. TRPV5-specific  $^{45}\text{Ca}^{2+}$  influx was determined by addition of 10  $\mu\text{M}$  ruthenium red (RR). (B) Representative trace of intracellular  $\text{Ca}^{2+}$  upon PTH stimulation using yellow cameleon 2.1 as a FRET sensor. (C) Basal calibrated  $\text{Ca}^{2+}$  levels in HEK293 cells transfected with mock ( $n = 8$ ) and TRPV5 ( $n = 9$ ). \* $P < 0.05$  versus mock. (D) Average trace of intracellular  $\text{Ca}^{2+}$  levels of TRPV5 upon treatment with PTH ( $n = 9$ ). (Inset) Relative FRET  $\text{Ca}^{2+}$  increase from basal to PTH-stimulated conditions, as shown by time periods "A" and "B," respectively. \*Significant difference ( $P < 0.05$ ) from basal conditions.

ways in PTH-induced stimulation of renal  $\text{Ca}^{2+}$  reabsorption.<sup>5,7,11,12</sup>

The transient receptor potential vanilloid 5 (TRPV5)  $\text{Ca}^{2+}$  channel constitutes the apical entry gate for active (transcellular)  $\text{Ca}^{2+}$  reabsorption from the distal part of the nephron.<sup>13,14</sup> It is, therefore, a likely target of PTH. Support for this notion is provided by the observation that long-term exposure to PTH enhances TRPV5 activity *via* two distinct mechanisms. PTH increases TRPV5 expression<sup>15</sup> and causes accumulation of the channel at the plasma membrane. The latter effect involves PLC signaling and a subsequent PKC-dependent phosphorylation.<sup>16</sup> In contrast, the molecular target for the adenylyl cyclase–cAMP–protein kinase A (PKA) pathway activated by PTH has not been identified. Using *ex vivo* models of active  $\text{Ca}^{2+}$  reabsorption, PTH-induced cAMP signaling was demonstrated to be essential for rapid stimulation of luminal  $\text{Ca}^{2+}$  uptake.<sup>5,11,17,18</sup> Interestingly, primary cultures of isolated rabbit connecting tubules (CNT) and cortical collecting duct cells, which express endogenous TRPV5, displayed increased transcellular  $\text{Ca}^{2+}$  transport after exposure to forskolin or cAMP-elevating hormones, including PTH.<sup>12,19,20</sup> Thus, despite the large number of studies investigating the role of PTH in renal  $\text{Ca}^{2+}$  handling, the molecular mechanism connecting the cAMP pathway with subsequent stimulation of active  $\text{Ca}^{2+}$  reabsorption has not yet been determined. Because TRPV5 has several putative PKA phosphorylation sites and is fundamental to renal  $\text{Ca}^{2+}$  handling, this channel is a likely target for PTH stimulation *via* the cAMP-signaling pathway.

The aim of this study, therefore, was to elucidate the potential role of TRPV5 in PTH-induced stimulation of transcellular  $\text{Ca}^{2+}$  reabsorption *via* cAMP-PKA signaling. First, we confirmed that PTH increases  $^{45}\text{Ca}^{2+}$  influx in HEK293 cells co-

expressing TRPV5 and PTH1R. Next, after exposure to PTH we monitored intracellular  $\text{Ca}^{2+}$ , phosphatidylinositol-4,5-bisphosphate ( $\text{PIP}_2$ ) and cAMP levels in this model system by dynamic fluorescence resonance energy transfer (FRET) assays. Furthermore, we investigated the consequence of forskolin-induced cAMP elevation on TRPV5 function. Finally, we determined TRPV5 cell surface abundance and single channel activity after activation of the cAMP-PKA signaling cascade.

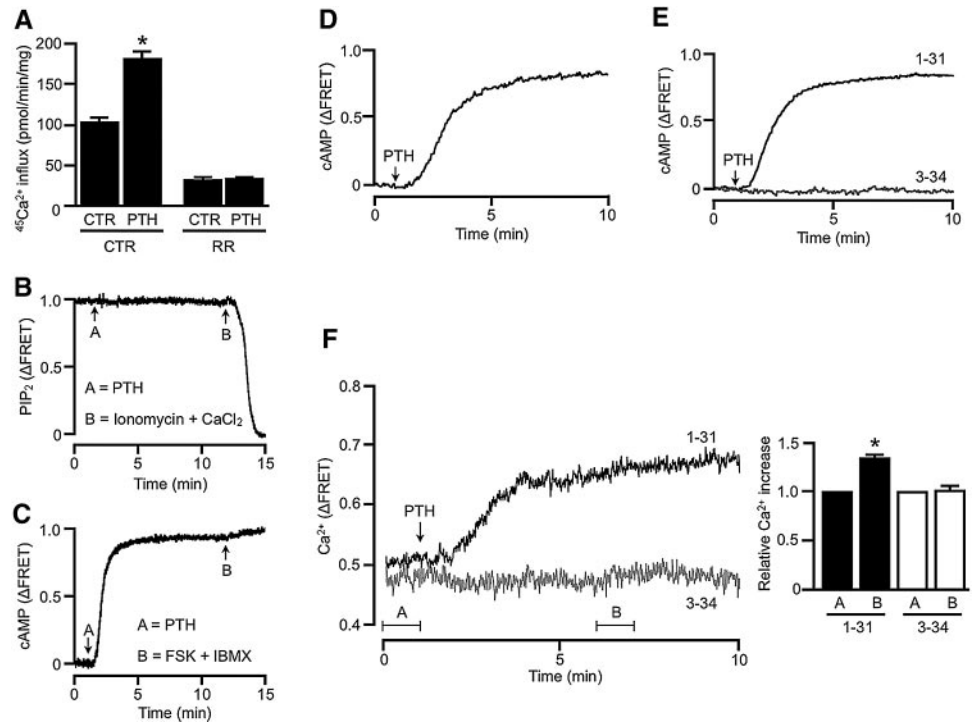
## RESULTS

### PTH Induces a Sustained Increase in TRPV5-Mediated $\text{Ca}^{2+}$ Influx

For studying the role of PTH on TRPV5 activity, TRPV5 and PTH1R were coexpressed in HEK293 cells and treated for 10 min with 10 nM PTH, and, subsequently, we determined the  $^{45}\text{Ca}^{2+}$  influx rate. Because TRPV5 is known to be rapidly inactivated by elevated intracellular  $\text{Ca}^{2+}$  levels,<sup>21</sup> we pretreated the cells with 25  $\mu\text{M}$  1,2-bis-(2-aminophenoxy)ethane-N,N,N',N'-tetra-acetic acid-acetoxymethyl ester (BAPTA-AM), a cell-permeable  $\text{Ca}^{2+}$  buffer. Under these conditions, we observed a significant enhancement of TRPV5 activity by PTH (Figure 1A). Ruthenium red, a selective blocker of TRPV5,<sup>22</sup> inhibited  $^{45}\text{Ca}^{2+}$  uptake under control and PTH-stimulated conditions (Figure 1A).

To measure the acute effect of PTH on TRPV5 function, HEK293 cells were transfected with yellow cameleon 2.1, a FRET sensor that detects free intracellular  $\text{Ca}^{2+}$ . Figure 1B shows a typical example of a calibrated FRET trace. FRET was normalized to a minimum value, obtained after addition of 4 mM BAPTA (point B) in combination with 5  $\mu\text{M}$  of the  $\text{Ca}^{2+}$

**Figure 2.** Dynamic effects of PTH and its fragments on PIP<sub>2</sub>, cAMP, and Ca<sup>2+</sup> levels. (A) <sup>45</sup>Ca<sup>2+</sup> uptake of HEK293 cells transiently coexpressing PTH1R and TRPV5-PKC6 was performed as previously performed with TRPV5-WT. \**P* < 0.05 versus CTR. (B) PIP<sub>2</sub> response upon PTH stimulation in cells coexpressing PIP<sub>2</sub> FRET sensors, PTH1R, and TRPV5-WT. (C) Consequence of PTH treatment on intracellular cAMP response. (D and E) Average cAMP trace upon stimulation of full-length PTH (*n* = 7; D) and PTH (1 to 31) (*n* = 10) and PTH (3 to 34) (*n* = 4; E). (F) Average FRET data representing intracellular Ca<sup>2+</sup> of cells expressing TRPV5-WT upon stimulation with PTH (1 to 31) (*n* = 9) and PTH (3 to 34) (*n* = 5). Ca<sup>2+</sup> levels during unstimulated (as depicted by "A") and forskolin-treated conditions (time period "B") for both PTH fragments, as shown by inset figure. \**P* < 0.05 versus basal conditions.



ionophore ionomycin (point C), and a maximum value was reached after addition (point D) of 8 mM CaCl<sub>2</sub>. These experiments revealed that basal intracellular Ca<sup>2+</sup> concentrations in HEK293 cells expressing wild-type TRPV5 (TRPV5-WT) were significantly higher than mock-transfected cells (Figure 1C). PTH stimulation of TRPV5-expressing cells resulted in a further steady increase of the intracellular Ca<sup>2+</sup> concentration, starting 40 to 50 s after addition of PTH and leveling off after approximately 3 min (Figure 1D). In the presence of PTH, the intracellular Ca<sup>2+</sup> concentration was significantly greater than under the control conditions, as shown in Figure 1D.

### PTH-Induced Activation of the cAMP Signaling Cascade Stimulates TRPV5

To study the role of PKC in PTH-dependent acute activation of TRPV5, we used a TRPV5 mutant lacking all six putative PKC consensus sites (TRPV5-PKC6)<sup>23</sup>. A previous study demonstrated that two of these PKC consensus sites play a crucial role in the PTH-induced accumulation of TRPV5 at the cell surface.<sup>16</sup> This long-term TRPV5 activation was shown to depend on PLC signaling and subsequent PIP<sub>2</sub> breakdown.<sup>23</sup> Interestingly, treatment of HEK293 cells coexpressing PTH1R and TRPV5-PKC6 with PTH enhanced <sup>45</sup>Ca<sup>2+</sup> influx to a similar extent as TRPV5-WT (Figure 2A). Because these results suggested the involvement of an alternative signaling pathway, we used FRET sensors for intracellular PIP<sub>2</sub><sup>24</sup> and cAMP.<sup>25</sup> Figure 2B depicts a typical FRET trace for the PIP<sub>2</sub> sensor under resting conditions (*t* = 0 min) and during maximal stimulation using 5 μM ionomycin and 8 mM CaCl<sub>2</sub> to activate Ca<sup>2+</sup>-dependent PLCs.<sup>26</sup> We did not detect PIP<sub>2</sub> breakdown after treatment with 10 nM PTH, using HEK293 cells with (*n* = 6)

or without (*n* = 4; data not shown) TRPV5 coexpression (Figure 2B). Using the Epac-based FRET sensor, the intracellular cAMP levels were monitored in PTH-stimulated HEK293 cells. A representative trace is presented in Figure 2C. The FRET results were expressed by normalizing traces between the resting value (at *t* = 0 min) and a maximum value, which was induced by treatment with 50 μM forskolin and 0.5 mM isobutylmethylxanthine. In Figure 2D, mean cAMP levels upon addition of PTH are depicted. PTH induced a rapid elevation of cAMP that reaches a plateau after 9 min. This stimulation was 80 to 90% of the maximum FRET values.

To study the involvement of the cAMP pathway in PTH-induced TRPV5 activation in more detail, we used different PTH fragments. The biologic active part of PTH is comprised by the first 34 amino acids. The first two residues of the N-terminus are required for a cAMP response.<sup>10</sup> Consistent with a PTH-specific elevation in cAMP levels PTH (1 to 31), in contrast to PTH (3 to 34), rapidly increased cAMP levels (Figure 2E). Compelling evidence for the crucial role of cAMP in TRPV5 activation was gained by measuring intracellular Ca<sup>2+</sup>. PTH (1 to 31) treatment induced a sustained raise of intracellular Ca<sup>2+</sup>, which reached a maximal effect after approximately 3 min (Figure 2F). In contrast, PTH (3 to 34) did not affect intracellular Ca<sup>2+</sup> concentrations (Figure 2F).

### Forskolin Mimics the PTH-Dependent Activation of TRPV5

We used forskolin to study directly the role of cAMP in the regulation of TRPV5 channel activity. We determined the influx of <sup>45</sup>Ca<sup>2+</sup> in HEK293 cells transiently expressing TRPV5 treated with 10 μM forskolin for 10 min. Forskolin signifi-

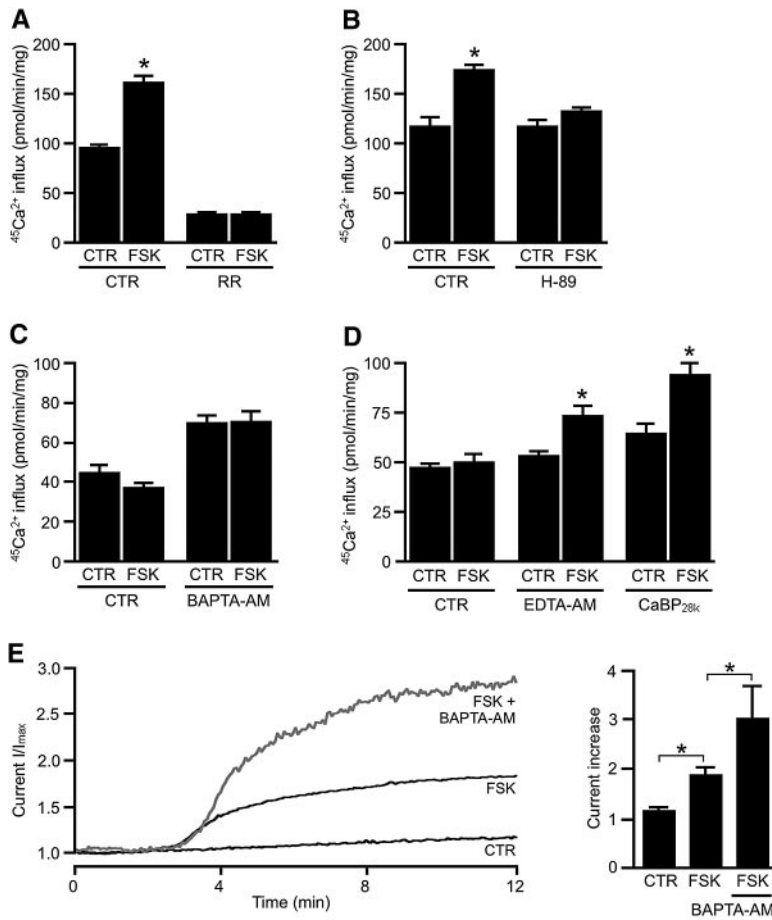


**Figure 3.** Forskolin (FSK) specifically stimulates TRPV5 activity under  $\text{Ca}^{2+}$ -chelating conditions. (A)  $^{45}\text{Ca}^{2+}$  uptake of HEK293 cells transiently expressing TRPV5 and pretreated for 30 min with 25  $\mu\text{M}$  BAPTA-AM. FSK was administered simultaneously with  $^{45}\text{Ca}^{2+}$ . (B) Potential role of PKA was investigated by 30 min of pretreatment of 10  $\mu\text{M}$  H-89. (C) FSK effect on  $^{45}\text{Ca}^{2+}$  uptake of HEK293 cells transiently expressing TRPV6, pretreated with 25  $\mu\text{M}$  BAPTA-AM and DMSO as a control. (D) Both pretreatment of 25  $\mu\text{M}$  EDTA-AM and coexpression of calbindin- $\text{D}_{28\text{K}}$  (CaBP $_{28\text{K}}$ ) enabled an FSK-induced stimulation of TRPV5 function. (E) Amphotericin B perforated whole-cell patch-clamp was used to study  $\text{Na}^{+}$  currents of cells expressing TRPV5-WT. At  $t = 2$  min, cells were treated with 10  $\mu\text{M}$  FSK. For investigation of the effect of intracellular  $\text{Ca}^{2+}$  on TRPV5 activity by FSK, cells were treated with 100  $\mu\text{M}$  BAPTA-AM. (Inset) Current increase of CTR ( $n = 8$ ), FSK ( $n = 10$ ), and FSK + BAPTA-AM ( $n = 11$ ) after 14 min compared with the current measured at  $t = 2$  min. \* $P < 0.05$  versus CTR.

cantly increased TRPV5 activity, fully mimicking PTH stimulation (Figure 3A). Again, ruthenium red blocked TRPV5-mediated  $^{45}\text{Ca}^{2+}$  uptake under both control and forskolin-treated conditions (Figure 3A). Subsequently, we investigated the potential involvement of PKA in the activation of TRPV5, because forskolin is a widely known activator of this enzyme; therefore, HEK293 cells transiently expressing TRPV5 were pretreated for 30 min with 10  $\mu\text{M}$  H-89, a selective blocker of PKA activity.<sup>27</sup> This abolished the forskolin-induced stimulation of TRPV5 activity (Figure 3B). To determine the specificity of the PKA-mediated increase in TRPV5 activity, we used the closely related epithelial  $\text{Ca}^{2+}$  channel, TRPV6, known as the luminal entry gate for intestinal  $\text{Ca}^{2+}$  absorption.<sup>28</sup> Acute forskolin treatment did not alter TRPV6 activity in either the presence or the absence of buffers to chelate intracellular  $\text{Ca}^{2+}$  (Figure 3C), confirming that the forskolin-induced channel activation is specific for TRPV5.

Under conditions lacking an intracellular buffer for  $\text{Ca}^{2+}$ , forskolin did not noticeably affect TRPV5-mediated  $^{45}\text{Ca}^{2+}$  influx (Figure 3D). PTH also failed to increase  $^{45}\text{Ca}^{2+}$  influx under these conditions ( $40 \pm 5$  and  $46 \pm 6$  pmol/min per mg for control and PTH, respectively;  $P > 0.2$ ). Next, we used EDTA-acetoxymethyl ester (EDTA-AM), a buffer with relatively slow  $\text{Ca}^{2+}$ -binding kinetics relative to BAPTA-AM,<sup>29</sup> to

study further the role of  $\text{Ca}^{2+}$  buffering in TRPV5 regulation by forskolin. Pretreatment with EDTA-AM and subsequent forskolin stimulation increased TRPV5 activity, although less pronounced compared with BAPTA-AM pretreatment (Figure 3D). Importantly, the  $\text{Ca}^{2+}$ -binding protein calbindin- $\text{D}_{28\text{K}}$ , which co-localizes with TRPV5 in renal tubular epithelial cells,<sup>30,31</sup> acts as a natural cytosolic  $\text{Ca}^{2+}$  buffer. The coexpression of calbindin- $\text{D}_{28\text{K}}$  in HEK293 cells also permitted a significant increase of  $^{45}\text{Ca}^{2+}$  influx upon forskolin treatment (Figure 3D).

Next, we investigated the role of intracellular  $\text{Ca}^{2+}$  on forskolin-induced activation of TRPV5 using patch-clamp analysis. Forskolin did not alter TRPV5-mediated  $\text{Na}^{+}$  currents in the ruptured whole-cell mode (Supplemental Figure 1); therefore, we further investigated TRPV5 regulation by amphotericin B-perforated patch-clamp analysis. In this configuration, forskolin rapidly elevated whole-cell  $\text{Na}^{+}$  currents (Figure 3E). Subsequently, we treated cells with BAPTA-AM. In comparison with untreated conditions, BAPTA-AM treatment did not significantly increase the basal  $\text{Na}^{+}$  current ( $106 \pm 5\%$ ;  $n = 13$ ;  $P > 0.2$ ), indicating that the basal intracellular  $\text{Ca}^{2+}$  concentration does not inhibit TRPV5 activity. Importantly, BAPTA-AM pretreatment amplified the forskolin-mediated stimulation of TRPV5 (Figure 3E).



### PKA-Mediated TRPV5 Stimulation Depends on Threonine Residue 709

Next, we inquired whether the forskolin-mediated TRPV5 stimulation was due to a direct phosphorylation of the channel by PKA. To identify putative PKA consensus sites in TRPV5, we used the prediction server NetPhosk (<http://www.cbs.dtu.dk/services>). Computational analysis of the TRPV5 amino acid sequence of four different mammalian species resulted in the identification of three highly conserved PKA consensus sites (Figure 4A). Of the putative phospho-residues, one serine was located in the N-tail (S142), whereas the C-tail harbored the other putative sites, another serine and a threonine residue (S680 and T709). Using site-directed mutagenesis, each residue was substituted for an alanine. Replacement of the T709 residue with alanine abolished forskolin-stimulated  $^{45}\text{Ca}^{2+}$  uptake, whereas mutation of S142 or S680 did not prevent the TRPV5 activation by forskolin (Figure 4B). Again, forskolin stimulation of TRPV5-PKC6 did not differ from stimulation of TRPV5-WT (Figure 4B). Importantly, TRPV5 protein expression was not affected by the introduction of these mutations (Figure 4C). The essential role of T709 in forskolin-induced TRPV5 activation was further supported by perforated patch analysis (Supple-

mental Figure 2) and FRET analysis (Figure 4D). Forskolin significantly increased the intracellular  $\text{Ca}^{2+}$  concentration of cells expressing TRPV5-WT; however, no effect was observed for TRPV5-T709A (Figure 4D). Likewise, TRPV5 activation by PTH also required an intact T709 phosphorylation site (Supplemental Figure 3).

To confirm the crucial role of T709 in PKA-mediated TRPV5 stimulation, we performed *in vitro* phosphorylation experiments using the amino (N)- or carboxyl (C)-tail of TRPV5 fused to glutathione S-transferase (GST). Proteins were incubated for 30 min in the presence of [ $\gamma^{32}\text{P}$ ]ATP and the purified catalytic subunit of PKA. Equal loading was verified by Coomassie staining, as shown in the Figure 4E, top. Robust  $^{32}\text{P}$ -phosphorylation was detected for the GST C-tail, whereas no radioactivity was present for the GST N-tail or for GST alone (Figure 4E). In contrast to  $^{32}\text{P}$  labeling of GST C-tail harboring the S680A mutation, substitution of T709 by alanine significantly reduced  $^{32}\text{P}$  labeling of the C-tail, confirming the critical role of T709.

### Molecular Mechanism of PKA-Induced TRPV5 Activity

We next addressed the molecular mechanism mediating the rapid increase of TRPV5 activity upon forskolin treatment. To

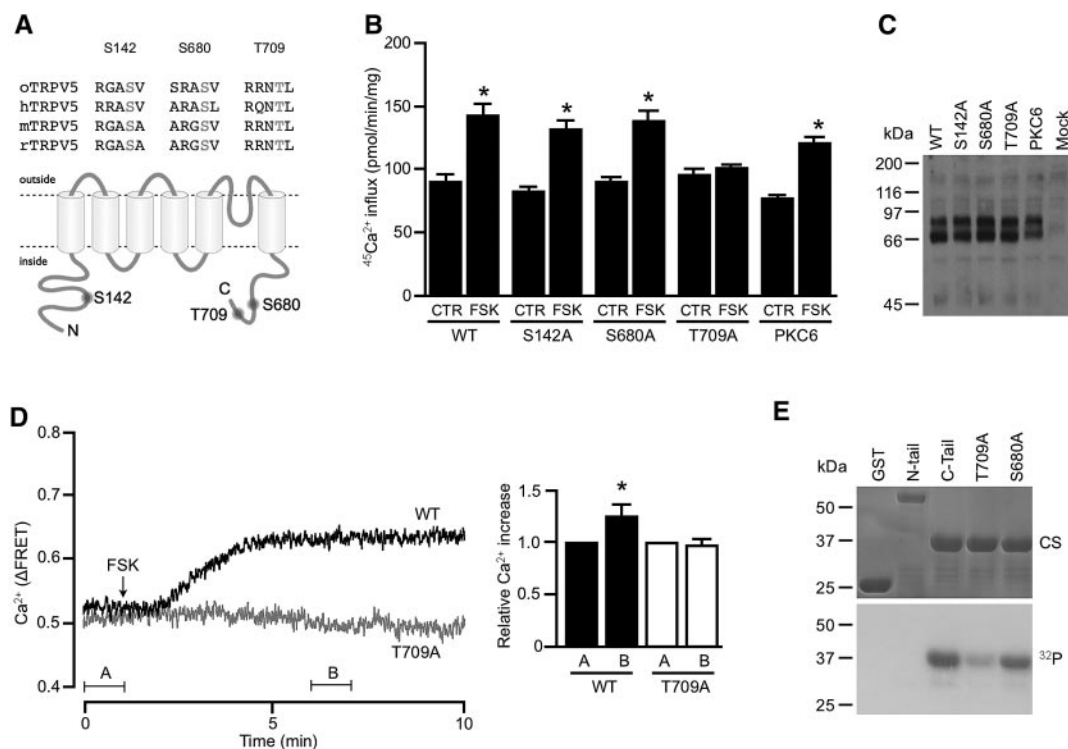


**Figure 4.** Threonine 709 is necessary for forskolin-induced TRPV5 stimulation. (A) Localization of putative PKA phosphorylation sites within several TRPV5 species. (B) Putative phosphorylation residues S142, S680, and T709 of TRPV5 were individually mutated into alanine.  $^{45}\text{Ca}^{2+}$  uptake of HEK293 cells expressing TRPV5-WT, TRPV5 point mutants, or TRPV5-PKC6 was conducted in the presence of 25  $\mu\text{M}$  BAPTA-AM. \* $P < 0.05$  versus CTR. (C) Protein expression of TRPV5-WT and mutants. (D) Average calibrated FRET  $\text{Ca}^{2+}$  levels of TRPV5-WT (black trace,  $n = 9$ ) and TRPV5-T709A (gray trace,  $n = 5$ ), both stimulated with forskolin. (Inset) Comparison of basal  $\text{Ca}^{2+}$  levels (time period "A") and  $\text{Ca}^{2+}$  levels after forskolin stimulation ("B") of TRPV5-WT and TRPV5-T709A. \* $P < 0.05$  versus basal conditions. (E) *In vitro* phosphorylation of TRPV5 N- and C-tail fused to GST. (Top) Protein input via Coomassie staining. (Bottom)  $^{32}\text{P}$  radiation.

this end, we pretreated HEK293 cells expressing TRPV5-WT or TRPV5-T709A with 25  $\mu$ M BAPTA-AM, stimulated them for 10 min with forskolin, and subjected them to cell surface biotinylation. Cells were lysed, and biotinylated proteins were precipitated with neutravidin-agarose beads. Using immunoblotting, TRPV5 expression in total cell lysates and plasma membrane fraction was determined as depicted by Figure 5, A and B, respectively. Forskolin treatment did not affect the cell surface expression of TRPV5 (Figure 5B), suggesting that an alteration in the single-channel activity of a fixed number of channels is responsible for the PTH-mediated increase in TRPV5 activity.

TRPV5 channel activity, therefore, was measured with the cell-attached patch-clamp technique. Using HEK293 cells transiently expressing TRPV5, we attached the patch pipette to the cell without disrupting the membrane, and we recorded TRPV5 channel current using  $\text{Na}^+$  as a charge carrier. As previously reported,<sup>32</sup> virtually no channel activity was observed at positive membrane potentials (Figure 6A). The current-voltage (I-V) relationship established in response to a voltage ramp from  $-100$  to  $80$  mV revealed an average single-channel conductance of  $90 \pm 11$  pS ( $n = 7$ ). Such channel activity was not present in nontransfected cells. Amplitude histogram analysis of the  $-80$  mV recording revealed the presence of two channels in the patch (Figure 6A). Having established a stable recording of TRPV5 channel current at  $-80$  mV, we added forskolin to the bath solution. TRPV5 activity is represented by averaged data of channel open probability (NPo,  $n =$  number of channels,  $P_o =$  open probability of channel) of 5-s intervals. Forskolin application increased NPo values, which reached a

maximal effect 2 min after addition (Figure 6B). Subsequently, we compared mean NPo data during control conditions (min 0 to 1) and after forskolin addition (min 3 to 4). Representative channel openings of TRPV5-WT and TRPV5-T709A are depicted in Figure 6, C and D, respectively. During control conditions, channel activity of TRPV5-WT and TRPV5-T709A was not significantly different; however, the number of TRPV5-WT channel openings was increased during forskolin treatment (Figure 6E), whereas TRPV5-T709A was not affected (Figure 6F).

To investigate whether phosphorylation directly influences TRPV5 single-channel activity, we used inside-out single-channel patch-clamp analysis. Channel activity was restricted to recordings at negative potentials (Figure 7A). From the current-voltage (I-V) relationship, we calculated an average channel conductance of  $39 \pm 2$  pS. Amplitude histogram analysis of the  $-80$  mV recording revealed the presence of a single channel in the patch (Figure 7A). The effect of PKA was tested at a holding potential of  $-80$  mV. After excision of the plasma membrane, 1 mM ATP and 250 U/ml catalytic PKA were cumulatively added to the patch-clamp recording chamber. Application of the PKA subunit increased TRPV5-WT single-channel activity (Figure 7, B and D), whereas TRPV5-T709A single-channel activity was not significantly altered (Figure 7, C and E).

## DISCUSSION

This study delineates the molecular mechanism responsible for TRPV5 channel activation by PTH. HEK293 cells coexpressing TRPV5 and PTH1R demonstrated elevated cAMP levels upon the addition of PTH and a subsequent increase in cytosolic  $\text{Ca}^{2+}$ . This latter finding was due to enhanced TRPV5 activity. Activation of the cAMP-PKA pathway, using PTH (1 to 31) or forskolin, mimicked completely the PTH stimulation. Both sufficient  $\text{Ca}^{2+}$  buffering and PKA function were necessary for this increased TRPV5-mediated  $\text{Ca}^{2+}$  influx. A PKA-dependent phosphorylation of T709 was found to be essential for TRPV5 activation by PTH or forskolin. Finally, PTH-induced TRPV5 activity was not due to an increase in the number of functional channels at the plasma membrane but instead was found to be the result of an enhanced single-channel open probability of a fixed number of TRPV5 channels at the cell surface.

To our knowledge, this is the first study providing a molecular model linking the well-established role for cAMP-PKA signaling after PTH1R engagement to the stimulation of  $\text{Ca}^{2+}$  reabsorption from the pro-urine in the distal part of the nephron. Whereas the majority of  $\text{Ca}^{2+}$  reabsorption takes place in the proximal tubule and thick ascending limb of Henle *via* passive paracellular transport, only approximately 15% is actively reabsorbed in DCT and CNT<sup>33</sup>; however these last two nephron segments control the renal excretion of  $\text{Ca}^{2+}$  and are the target of PTH, which activates the cAMP signaling

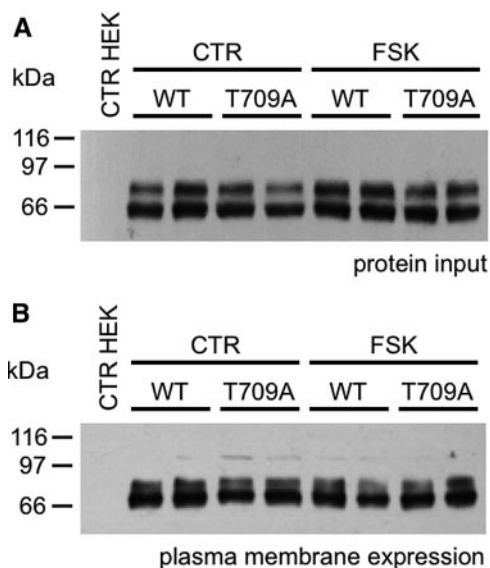


**Figure 5.** Forskolin does not affect TRPV5 cell surface abundance. Biotinylation studies were performed with HEK293 cells expressing TRPV5 pretreated with BAPTA-AM to chelate intracellular  $\text{Ca}^{2+}$ . (A and B) Forskolin had no effect on protein input (A) or plasma membrane expression (B) of TRPV5-WT or TRPV5-T709A.

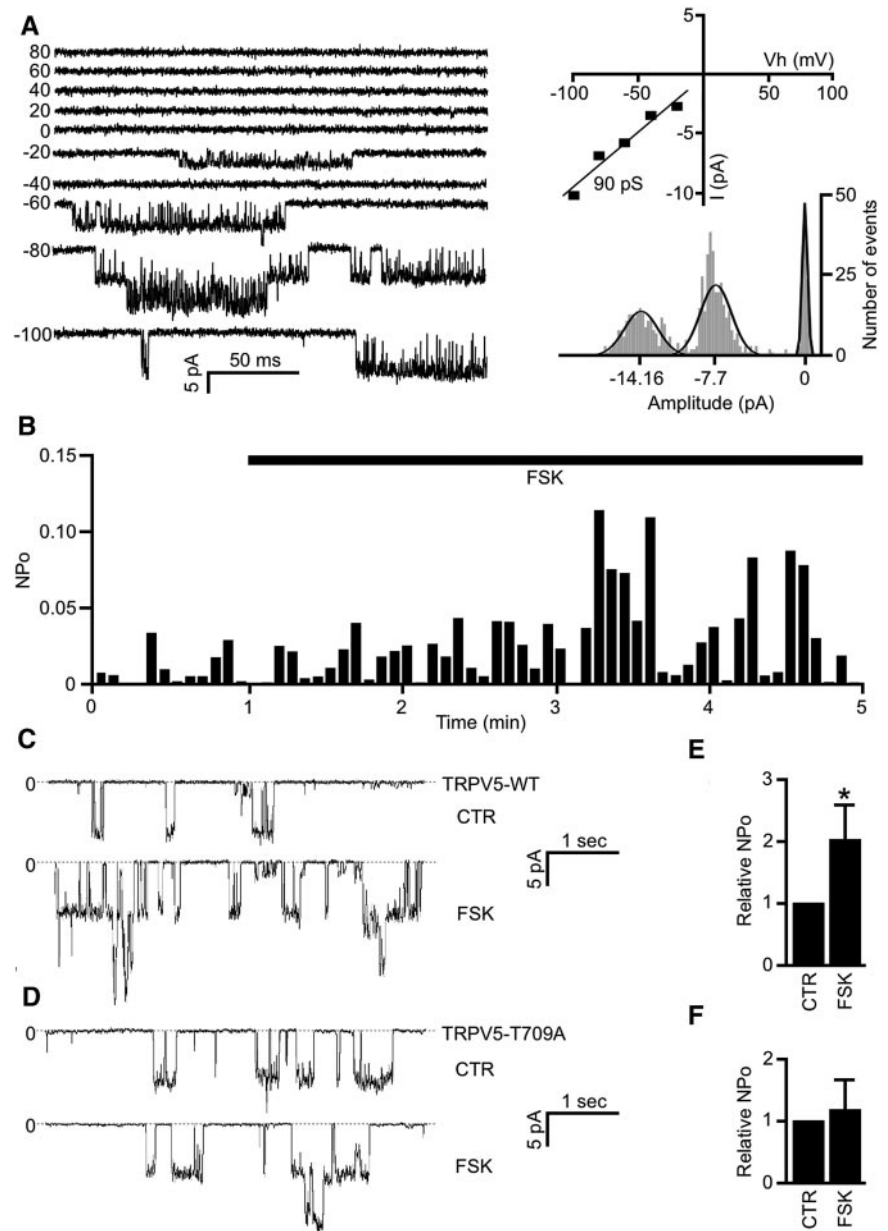


**Figure 6.** Forskolin stimulates TRPV5 channel activity. (A) Cell-attached single-channel recordings were made from HEK293 cells expressing TRPV5-WT. Channel activity was elicited by step potentials varying from  $-100$  to  $80$  mV (left). The averaged calculated slope conductance was  $90$  pS (top right). Amplitude histograms were constructed from regions of the single-channel recordings obtained at  $-80$  mV (bottom right). The histograms were fit by three Gaussian functions corresponding to a closed, one open, and two open levels. (B) Representative recording of TRPV5-WT in time using cell-attached patch-clamp (holding potential  $-80$  mV). NPo values were the average of 5-s intervals. (C and D) Representative channel openings of TRPV5-WT (C) and TRPV5-T709A (D) stimulated with forskolin. (E and F) Statistical analysis demonstrates a significant elevation for TRPV5-WT ( $n = 8$ ; E), whereas TRPV5-T709A channel activity ( $n = 8$ ; F) was not affected.  $*P < 0.05$  versus CTR.

cascade, eventually enhancing  $\text{Ca}^{2+}$  reabsorption.<sup>11,18,34,35</sup> Use of the adenylyl cyclase-activating compound, forskolin, and cell-permeable cAMP analogs in *ex vivo* models of active  $\text{Ca}^{2+}$  reabsorption mimicked the stimulatory effect of PTH.<sup>11,17,19,20,36,37</sup> Several studies suggested that PTH positively influences the uptake of  $\text{Ca}^{2+}$  from the pro-urine, although the specific protein mediating the apical influx of  $\text{Ca}^{2+}$  was unknown.<sup>5,17,18</sup> In 1999, Hoenderop *et al.*<sup>38</sup> identified TRPV5 as the apical uptake mechanism for active  $\text{Ca}^{2+}$  reabsorption in DCT and CNT. Functional analysis of TRPV5 knockout mice supported this notion, because the mean  $\text{Ca}^{2+}$  delivery to puncturing sites in DCT was significantly higher than wild-type mice.<sup>13</sup> These findings suggest that TRPV5 is the molecular target of PTH-induced  $\text{Ca}^{2+}$  reabsorption from the distal part of the nephron. Using

HEK293 cells coexpressing TRPV5 and PTH1R, we were able to reproduce the cAMP-mediated stimulation of  $\text{Ca}^{2+}$  influx upon the addition of PTH, as is observed in native tissue (*i.e.*, the kidney).

Buffering intracellular  $\text{Ca}^{2+}$  was found to be crucial for an increased TRPV5-mediated  $^{45}\text{Ca}^{2+}$  influx by forskolin. Interestingly, no additional buffer for  $\text{Ca}^{2+}$  was required for TRPV5 stimulation in the FRET assays. This is likely due to the  $\text{Ca}^{2+}$ -chelating effect of calmodulin residing in the yellow cameleon 2.1.<sup>39</sup> In contrast to EDTA-AM pretreatment, the addition of BAPTA-AM increased  $^{45}\text{Ca}^{2+}$  uptake of cells not stimulated with forskolin. This finding is in line with the fast binding kinetics of BAPTA compared with EDTA.<sup>29,40</sup> Both EDTA-AM and BAPTA-AM allowed TRPV5 activation by forskolin. Thus, in contrast to other ion channels, fast  $\text{Ca}^{2+}$  buffering is not



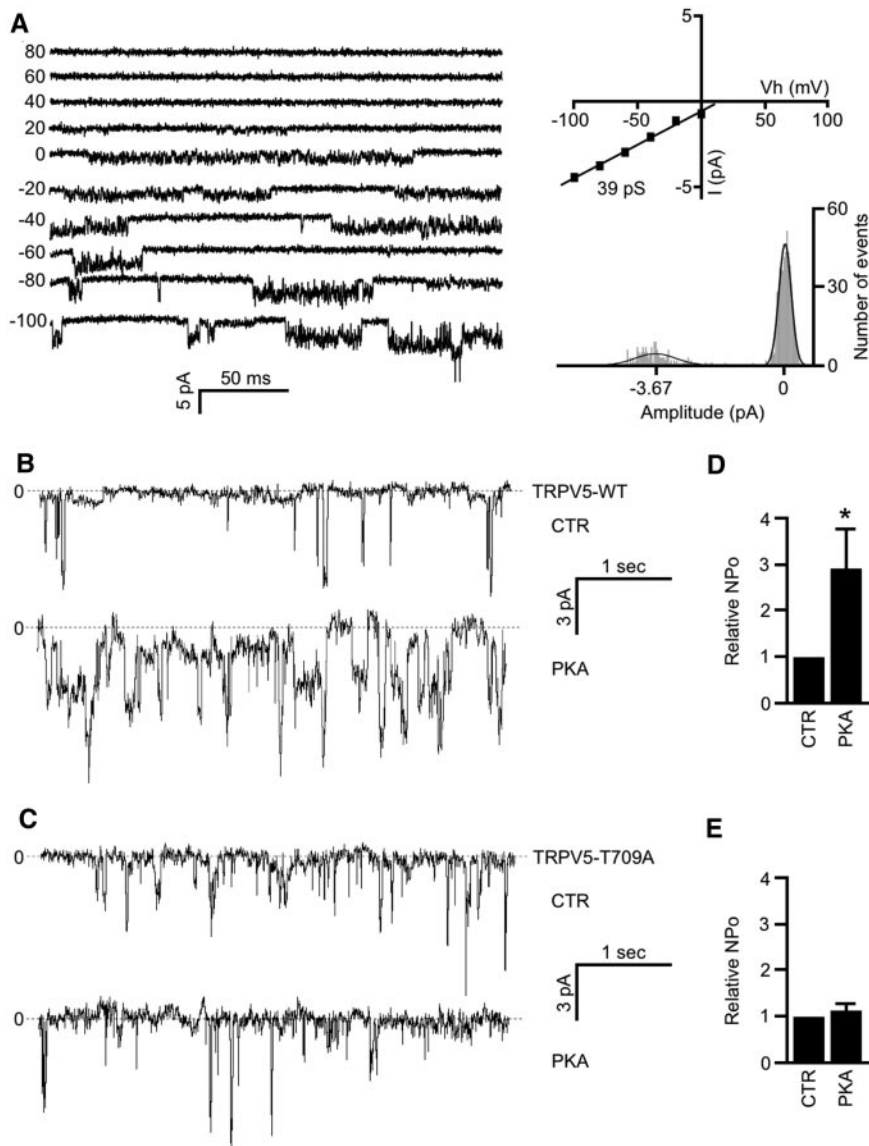


**Figure 7.** Isolated PKA catalytic subunit directly activates TRPV5-WT and not TRPV5-T709A. (A) The plasma membrane was excised when channel activity was detected in cell-attached configuration. Channel activity was elicited by step potentials varying from  $-100$  to  $80$  mV (left). Slope conductances of TRPV5 channels were obtained from single-channel current-voltage (I-V) relationship (top right). Amplitude histogram of single-channel recordings at  $-80$  mV is shown (bottom right). The histograms were fit by two Gaussian functions corresponding to a closed and one open level. (B and C) Representative current traces from inside-out patch of TRPV5-WT (B) and TRPV5-T709A (C) in response to  $-80$  mV holding potential. Inside-out patch was performed in the presence of  $1$  mM ATP and isolated PKA catalytic subunit. (D and E) Relative average NPo of TRPV5-WT ( $n = 7$ ; D) was increased after PKA catalytic subunit stimulation, whereas relative average NPo of TRPV5-T709A ( $n = 5$ ; E) was not significantly altered.  $*P < 0.05$  versus CTR.

crucial for TRPV5 activity. Coexpression of calbindin- $D_{28K}$  also buffered intracellular  $Ca^{2+}$  sufficiently to permit forskolin-induced TRPV5 stimulation. This  $Ca^{2+}$ -binding protein specifically co-localizes with TRPV5 in DCT and CNT and has been shown to play a crucial role in active  $Ca^{2+}$  reabsorption *in vivo*.<sup>31,41</sup> At low intracellular  $Ca^{2+}$  concentration, calbindin- $D_{28K}$  moves to a position near the plasma membrane and binds directly to TRPV5. The associated calbindin- $D_{28K}$  tightly buffers TRPV5-mediated  $Ca^{2+}$  influx. Hereby, transcellular  $Ca^{2+}$  transport is stimulated as TRPV5 inactivation is prevented by the lowered intracellular  $Ca^{2+}$  concentration.<sup>31</sup> The observation that TRPV5 and calbindin- $D_{28K}$  co-localize to the apical region of DCT and CNT supports our finding that acute TRPV5 stimulation by PTH requires the local presence of a  $Ca^{2+}$ -binding protein.

PKA plays a crucial role in forskolin-mediated TRPV5 activation. This is confirmed by the abolishment of TRPV5 stimulation by H-89, a PKA blocker. The threonine at position 709

in TRPV5, a PKA consensus site, is essential for the activation of TRPV5 by this mechanism, as demonstrated by  $^{45}Ca^{2+}$  uptake, FRET imaging, and patch-clamp analysis. *In vitro*, PKA phosphorylation of the TRPV5 C-tail was virtually abolished upon alanine substitution of T709. The remaining minor radioactive signal of the T709A mutant could possibly be due to an additional PKA site. It is of interest that only the threonine residue is completely conserved in all studied species, whereas S142 and S680, the other putative phosphorylation sites, not involved in forskolin-mediated TRPV5 activation, were absent in nonmammalian species. Furthermore, amino acid alignment with the close homologue TRPV6 failed to reveal a conserved putative PKA consensus site in proximity to TRPV5-T709. Consistent with this, forskolin did not affect TRPV6 activity, confirming the specificity of TRPV5 activation. Interestingly, PTH likely does not effect the intestinal absorption of  $Ca^{2+}$ , in which TRPV6 is the proposed luminal influx mechanism for  $Ca^{2+}$ .<sup>42</sup>

Using cell surface biotinylation assays and patch-clamp analysis, the direct molecular mechanism responsible for PTH-induced TRPV5 activation was elucidated. Because forskolin-mediated PKA activation did not affect TRPV5 plasma membrane expression, we studied single-channel activity in the cell-attached and inside-out configuration. TRPV5 channel conductance (90 pS) in cell-attached patch-clamp analysis was similar to our previously published values.<sup>32</sup> In addition, inside-out recordings revealed an average conductance of 39 pS, which is slightly lower than the previously reported values.<sup>32,43</sup> In our collaborative study with Nilius *et al.*,<sup>32</sup> we demonstrated variability in the single-channel conductance ranging from 55 to 95 pS. Use of different solutions and pH in the individual reports might provide an explanation for the differences in channel conductance between these studies.<sup>43</sup> Using the cell-attached as well as inside-out configuration TRPV5 single-channel activity was studied in response to forskolin and the catalytic PKA subunit. A significant increase in TRPV5 open probability was measured in both configurations, whereas channel activity of TRPV5-T709A was not altered. Thus, our data suggest that PTH augments the open probability of TRPV5 channels *via* a PKA-dependent phosphorylation, which in turn results in an increased TRPV5-mediated  $\text{Ca}^{2+}$  influx.

The stimulatory effect of PTH and forskolin on TRPV5 activity in HEK293 cells was detected only at low intracellular  $\text{Ca}^{2+}$  concentrations. Thus, PKA-mediated TRPV5 stimulation seems to rely on an unidentified  $\text{Ca}^{2+}$ -sensitive pathway. To investigate further the role of intracellular  $\text{Ca}^{2+}$  on TRPV5 stimulation by PKA, we initiated perforated patch-clamp recordings. TRPV5 activity was determined by measuring the whole-cell  $\text{Na}^+$  current. In contrast to the <sup>45</sup> $\text{Ca}^{2+}$  uptake assay, no additional  $\text{Ca}^{2+}$  buffering was required to observe TRPV5 stimulation by forskolin. The absence of  $\text{Ca}^{2+}$  influx *via* TRPV5 in this latter patch-clamp configuration prevents an increase in intracellular  $\text{Ca}^{2+}$  concentration and therefore allows stimulation of channel activity by forskolin. Subsequently, cells were treated with BAPTA-AM. In comparison with the control condition, BAPTA-AM treatment did not significantly increase the basal TRPV5-mediated  $\text{Na}^+$  current. This indicates that under these conditions, the basal intracellular  $\text{Ca}^{2+}$  concentration does not inhibit TRPV5 activity; however, BAPTA-AM pretreatment amplified the forskolin-mediated stimulation of TRPV5. In a previous study performed in MDCK cells stably expressing TRPV5, forskolin increased TRPV5-mediated  $\text{Ca}^{2+}$  influx without the presence of an additional  $\text{Ca}^{2+}$  buffer.<sup>44</sup> Differences in basal  $\text{Ca}^{2+}$  concentrations between TRPV5-expressing HEK293 and MDCK cells might provide an explanation for this observation. Further research is needed to identify the exact  $\text{Ca}^{2+}$ -sensitive pathway preventing TRPV5 stimulation at increased intracellular  $\text{Ca}^{2+}$  concentrations.

In addition to the  $\text{Ca}^{2+}$ -sensitive cAMP-PKA signaling pathway, PTH has been reported to affect TRPV5 function *via* other molecular mechanisms.<sup>13,45</sup> Several groups have demon-

strated that PKC is required for the PTH-mediated increase in  $\text{Ca}^{2+}$  reabsorption.<sup>12,46</sup> Recently, Cha *et al.*<sup>16</sup> confirmed the crucial role of PLC-PKC signaling in PTH-induced TRPV5 stimulation. Activation of the PKC pathway reduced caveolae-mediated TRPV5 endocytosis, resulting in an increased channel activity<sup>16</sup>; therefore, a 15-min pretreatment with PTH was required. Furthermore, the TRPV5 channel lacking both PKC phosphorylation sites did not respond to PTH.<sup>16</sup> Interestingly, in our experiments, PTH stimulation of the TRPV5 channel missing these PKC sites was identical to TRPV5-WT. These distinctive data might result from differences in the experimental setup. Cha *et al.*<sup>16</sup> applied 120 nM PTH for 15 min to activate a PKC-signaling pathway, whereas we demonstrated TRPV5 channel activity with 10 nM PTH within 5 min, suggesting that moderate stimulation of PTH1R fully triggers the cAMP-PKA pathway.

In 2005, van Abel *et al.*<sup>15</sup> demonstrated that PTH upregulates TRPV5 expression, which increases active  $\text{Ca}^{2+}$  reabsorption *via* a long-term manner. Parathyroidectomized rats displayed a downregulation of TRPV5 protein expression, whereas long-term PTH supplementation restored the expression. Thus, besides stimulating TRPV5 protein expression and plasma membrane localization, PTH rapidly elevates TRPV5 channel activity, highlighting the essential role for PTH as the *in vivo* mediator of renal  $\text{Ca}^{2+}$  sparing.

Altogether, our results suggest that TRPV5 is the molecular target for the rapid PTH-induced stimulation of active  $\text{Ca}^{2+}$  reabsorption in the distal part of the nephron. Activation of PTH1R initiates a signaling pathway, which involves cAMP and PKA that eventually results in the phosphorylation of threonine 709 and a subsequent increase in TRPV5 single-channel activity.

## CONCISE METHODS

### Molecular Biology and Cell Culture

Constructs containing TRPV5, TRPV6, or calbindin-D<sub>28K</sub> in pCINEO/IRES-GFP were obtained as described previously.<sup>47</sup> Single PKA mutants were generated by alanine substitution of the threonine and serine residues of putative phosphorylation sites of TRPV5 (S142A, S680A, and T709A) using *in vitro* mutagenesis. TRPV5 N- and C-tail were cloned into the pGEX 6p-2 vector; subsequently, the previously described putative phosphorylation sites of TRPV5 were mutated into an alanine. The FRET sensor for  $\text{Ca}^{2+}$  (yellow cameleon 2.1) was a gift of Dr. Tsien (University of California, San Diego, La Jolla, CA). FRET sensors for cAMP, CFP-Epac-YFP,<sup>25</sup> PIP<sub>2</sub>, eCFP-PH $\delta$ 1, and eYFP $\delta$ 1 were generated as described previously.<sup>24</sup> For the combined use of TRPV5 and both FRET sensors, IRES-GFP was removed from the original pCINEO/IRES-GFP vector. The PTH1R was a gift of Dr. Silver (Jerusalem, Israel). HEK293 cells were grown and transfected as described previously.<sup>48</sup> HEK293 cells stably expressing TRPV5 were generated as described previously<sup>44</sup> and maintained in medium containing 400  $\mu\text{g}/\text{ml}$  G418.

### <sup>45</sup>Ca<sup>2+</sup> Uptake

Radioactive Ca<sup>2+</sup> uptake was determined using TRPV5- and TRPV6-expressing HEK293 cells seeded in poly-L-lysine-coated (Sigma, St. Louis, MO) 24-well plates. Cells were pretreated for 30 min with 25  $\mu$ M BAPTA-AM or 25  $\mu$ M EDTA-AM, subsequently incubated for 5 min in KHB buffer (110 mM NaCl, 5 mM KCl, 1.2 mM MgCl<sub>2</sub>, 0.1 mM CaCl<sub>2</sub>, 10 mM Na-acetate, 2 mM NaH<sub>2</sub>PO<sub>4</sub>, and 20 mM HEPES [pH 7.4]-NaOH), and finally incubated for 10 min with <sup>45</sup>CaCl<sub>2</sub> (1  $\mu$ Ci/ml) in KHB buffer with voltage-gated Ca<sup>2+</sup> channel inhibitors (10  $\mu$ M flunarilol and 10  $\mu$ M verapamil). For blocking of TRPV5-mediated <sup>45</sup>Ca<sup>2+</sup> uptake, cells were incubated with 10  $\mu$ M ruthenium red during the 5- and 10-min incubation steps. After multiple washing steps with ice-cold stop buffer (110 mM NaCl, 5 mM KCl, 1.2 mM MgCl<sub>2</sub>, 10 mM Na-acetate, 0.5 mM CaCl<sub>2</sub>, 1.5 mM LaCl<sub>3</sub>, and 20 mM HEPES [pH 7.4]-NaOH), the uptake of <sup>45</sup>Ca<sup>2+</sup> was measured.

### Cell Surface Biotinylation and Immunoblotting

HEK293 cells stably expressing TRPV5 were seeded on poly-L-lysine-coated 10-cm dishes and treated similar as <sup>45</sup>Ca<sup>2+</sup> uptake assay. After 10 min of incubation with forskolin or ethanol (solvent) as a control, cells were placed on ice to inhibit intracellular trafficking processes. Subsequent biotinylation was performed on ice using 0.5 mg/ml sulfo-NHS-LC-LC-biotin (Pierce, Etten-leur, Netherlands) in PBS supplemented with 0.5 mM CaCl<sub>2</sub> and 1.0 mM MgCl<sub>2</sub> (PBS-CM) for 30 min. Unbound biotin was quenched with 0.1% (wt/vol) BSA in PBS-CM. Finally, cells were washed with PBS-CM and PBS and lysed in 150 mM NaCl, 5 mM EDTA, 50 mM Tris-HCl (pH 7.5), 1% (vol/vol) NP-40, 1 mM PMSF, 10  $\mu$ g/ml leupeptin, and 10  $\mu$ g/ml pepstatin A at 4°C. The lysate was centrifuged at 16,000  $\times$  g, and biotinylated proteins were precipitated *via* neutravidin-coupled beads (Pierce) and analyzed by immunoblot using anti-TRPV5 antibody.

### GST Pull-down and In Vitro Phosphorylation

TRPV5 C- and N-tails fused to GST were purified as described previously.<sup>49</sup> The precipitated fusion proteins, immobilized on glutathione Sepharose 4B beads, were incubated for 30 min at 30°C in kinase reaction buffer (50 mM Tris-HCl [pH 7.5], 10 mM MgCl<sub>2</sub>, and 100  $\mu$ M ATP) containing the catalytic subunit of PKA (100 U/ $\mu$ l reaction buffer; New England Biolabs, Leusden, The Netherlands) and 2  $\mu$ Ci of [ $\gamma$ <sup>32</sup>P]ATP. For removing unbound [ $\gamma$ <sup>32</sup>P]ATP, the beads were washed three times with 50 mM HEPES (pH 7.4)-KOH, 4 mM MnCl<sub>2</sub>, and 0.5 mM CaCl<sub>2</sub>. Proteins were eluted with SDS-PAGE loading buffer and separated on SDS-polyacrylamide gel, and *in vitro* phosphorylation was analyzed by autoradiography.

### Dynamic FRET Assays

Cells grown on glass coverslips (diameter 24 mm) were transfected with FRET constructs (1  $\mu$ g per coverslip), and experiments were performed as described previously.<sup>24,25</sup> In brief, coverslips were placed on an inverted Nikon microscope (Düsseldorf, Germany) and excited at 425 nm using an ND3 filter. CFP and YFP emission was collected simultaneously through 470  $\pm$  20- and 530  $\pm$  25-nm band-pass filters. Data were acquired at two samples per second, and FRET was expressed as ratio of CFP to YFP signals. Calibration of CFP/YFP

was accomplished by assessment of upper and lower saturation levels of the FRET sensors, resulting in  $\Delta$ FRET.

### Electrophysiology

Patch-clamp experiments in the single-channel mode and perforated whole-cell configuration were performed as described previously<sup>32</sup> at room temperature using an EPC-9 patch-clamp amplifier computer controlled by the Pulse software (HEKA Elektronik, Lambrecht, Germany). For single-channel measurements in cell-attached mode, cells were perfused with the following solution: 140 mM KCl, 5 mM EDTA, 5 mM EGTA, 1 mM MgCl<sub>2</sub>, 10 mM glucose, and 10 mM HEPES (pH 7.2)-KOH. For inside-out patches, excision was done in the same solution and 1 mM ATP was added. In both configurations, the pipette contained 140 mM NaCl, 10 mM EGTA, and 10 mM HEPES (pH 7.2)-NaOH. The sampling rate was 10 kHz; currents were filtered at 1 kHz. The analysis of single-channel data was performed using TAC software (Bruxon, Seattle, WA). Perforated whole-cell patch-clamp analysis was performed as described previously.<sup>50</sup> For perforated patch recordings, 0.6 mg/ml of the pore-forming agent amphotericin B was added to the following pipette solution: 100 mM Cs-Aspartate, 20 mM CsCl, 1 mM MgCl<sub>2</sub>, and 10 mM HEPES (pH 7.2)-CsOH. Cells were kept and recorded in nominal divalent-free solution containing 150 mM NaCl, 6 mM CsCl, 1 mM CaCl<sub>2</sub>, 1 mM MgCl<sub>2</sub>, 10 mM HEPES, and 10 mM glucose (pH 7.4)-NaOH. The action of amphotericin B was visible as a continuous decrease in serial resistance. Recordings were started when the serial resistance attained values below 15 M $\Omega$ . BAPTA-AM (100  $\mu$ M) was used to chelate intracellular free Ca<sup>2+</sup>, after which forskolin (10  $\mu$ M) was added. Perforated whole-cell data were analyzed using Igor pro software (Wave-metrics, Lake, Oswego, OR).

### Compounds

Full-length human PTH, human PTH (1 to 31), and bovine PTH (3 to 34) were purchased from Bachem AG (Bubendorf, Switzerland). Forskolin, amphotericin B, and the PKA inhibitor H-89 were purchased from Sigma.

### Statistical Analysis

In all experiments, data are expressed as means  $\pm$  SEM. Overall statistical significance was determined by ANOVA. In case of significance, differences between the means of two groups were analyzed by paired and unpaired *t* test. *P* < 0.05 was considered significant.

### ACKNOWLEDGMENTS

This work was financially supported in part by grants from the Dutch Kidney Foundation (C03.6017 and C06.2170) and The Netherlands Organization for Scientific Research (NWO-ALW 814.02.001, NWO-CW 700.55.302, and ZonMw 9120.6110). J.G.J.H. is supported by a EURYI award.

We thank Dr. T. Alexander, Dr. S. Verkaar, and H. Dimke for stimulating discussions and critical reading of the manuscript.



## DISCLOSURES

None.

## REFERENCES

- Case RM, Eisner D, Gurney A, Jones O, Muallem S, Verkhatsky A: Evolution of calcium homeostasis: From birth of the first cell to an omnipresent signalling system. *Cell Calcium* 42: 345–350, 2007
- Bootman MD, Collins TJ, Peppiatt CM, Prothero LS, MacKenzie L, De Smet P, Travers M, Tovey SC, Seo JT, Berridge MJ, Ciccolini F, Lipp P: Calcium signalling: An overview. *Semin Cell Dev Biol* 12: 3–10, 2001
- Brown EM: The calcium-sensing receptor: Physiology, pathophysiology and CaR-based therapeutics. *Subcell Biochem* 45: 139–167, 2007
- Garrett JE, Capuano IV, Hammerland LG, Hung BC, Brown EM, Hebert SC, Nemeth EF, Fuller F: Molecular cloning and functional expression of human parathyroid calcium receptor cDNAs. *J Biol Chem* 270: 12919–12925, 1995
- Lau K, Bourdeau JE: Parathyroid hormone action in calcium transport in the distal nephron. *Curr Opin Nephrol Hypertens* 4: 55–63, 1995
- Schwindinger WF, Fredericks J, Watkins L, Robinson H, Bathon JM, Pines M, Suva LJ, Levine MA: Coupling of the PTH/PTHrP receptor to multiple G-proteins: Direct demonstration of receptor activation of Gs, Gq/11, and Gi(1) by [ $\alpha$ -<sup>32</sup>P]GTP- $\gamma$ -azidoanilide photoaffinity labeling. *Endocrine* 8: 201–209, 1998
- Friedman PA, Gesek FA, Morley P, Whitfield JF, Willick GE: Cell-specific signaling and structure-activity relations of parathyroid hormone analogs in mouse kidney cells. *Endocrinology* 140: 301–309, 1999
- Sneddon WB, Magyar CE, Willick GE, Syme CA, Galbiati F, Bisello A, Friedman PA: Ligand-selective dissociation of activation and internalization of the parathyroid hormone (PTH) receptor: Conditional efficacy of PTH peptide fragments. *Endocrinology* 145: 2815–2823, 2004
- Donahue HJ, Fryer MJ, Eriksen EF, Heath H 3rd: Differential effects of parathyroid hormone and its analogues on cytosolic calcium ion and cAMP levels in cultured rat osteoblast-like cells. *J Biol Chem* 263: 13522–13527, 1988
- Whitfield JF, Isaacs R, MacLean S, Morley P, Barbier JR, Willick GE: Stimulation of membrane-associated protein kinase-C activity in spleen lymphocytes by hPTH-(1–31)NH<sub>2</sub>, its lactam derivative, [Leu<sup>27</sup>]-cyclo(Glu<sup>22</sup>-Lys<sup>26</sup>)-hPTH-(1–31)NH<sub>2</sub>, and hPTH-(1–30)NH<sub>2</sub>. *Cell Signal* 11: 159–164, 1999
- Shimizu T, Yoshitomi K, Nakamura M, Imai M: Effects of PTH, calcitonin, and cAMP on calcium transport in rabbit distal nephron segments. *Am J Physiol* 259: F408–F414, 1990
- Hoenderop JG, De Pont JJ, Bindels RJ, Willems PH: Hormone-stimulated Ca<sup>2+</sup> reabsorption in rabbit kidney cortical collecting system is cAMP-independent and involves a phorbol ester-insensitive PKC isotype. *Kidney Int* 55: 225–233, 1999
- Hoenderop JG, van Leeuwen JP, van der Eerden BC, Kersten FF, van der Kemp AW, Merillat AM, Waarsing JH, Rossier BC, Vallon V, Hummler E, Bindels RJ: Renal Ca<sup>2+</sup> wasting, hyperabsorption, and reduced bone thickness in mice lacking TRPV5. *J Clin Invest* 112: 1906–1914, 2003
- de Groot T, Bindels RJ, Hoenderop JG: TRPV5: An ingeniously controlled calcium channel. *Kidney Int* 74: 1241–1246, 2008
- van Abel M, Hoenderop JG, van der Kemp AW, Friedlaender MM, van Leeuwen JP, Bindels RJ: Coordinated control of renal Ca<sup>2+</sup> transport proteins by parathyroid hormone. *Kidney Int* 68: 1708–1721, 2005
- Cha SK, Wu T, Huang CL: Protein kinase C inhibits caveolae-mediated endocytosis of TRPV5. *Am J Physiol Renal Physiol* 294: F1212–F1221, 2008
- Lau K, Bourdeau JE: Evidence for cAMP-dependent protein kinase in mediating the parathyroid hormone-stimulated rise in cytosolic free calcium in rabbit connecting tubules. *J Biol Chem* 264: 4028–4032, 1989
- Lajeunesse D, Bouhtiaou I, Brunette MG: Parathyroid hormone and hydrochlorothiazide increase calcium transport by the luminal membrane of rabbit distal nephron segments through different pathways. *Endocrinology* 134: 35–41, 1994
- van Baal J, Raber G, de Slegte J, Pieters R, Bindels RJ, Willems PH: Vasopressin-stimulated Ca<sup>2+</sup> reabsorption in rabbit cortical collecting system: Effects on cAMP and cytosolic Ca<sup>2+</sup>. *Pflugers Arch* 433: 109–115, 1996
- Bindels RJ, Hartog A, Timmermans J, Van Os CH: Active Ca<sup>2+</sup> transport in primary cultures of rabbit kidney CCD: Stimulation by 1,25-dihydroxyvitamin D<sub>3</sub> and PTH. *Am J Physiol* 261: F799–F807, 1991
- Vennekens R, Hoenderop JG, Prenen J, Stuijver M, Willems PH, Droogmans G, Nilius B, Bindels RJ: Permeation and gating properties of the novel epithelial Ca<sup>2+</sup> channel. *J Biol Chem* 275: 3963–3969, 2000
- Nilius B, Prenen J, Vennekens R, Hoenderop JG, Bindels RJ, Droogmans G: Pharmacological modulation of monovalent cation currents through the epithelial Ca<sup>2+</sup> channel ECaC1. *Br J Pharmacol* 134: 453–462, 2001
- Gkika D, Topala CN, Chang Q, Picard N, Thebault S, Houillier P, Hoenderop JG, Bindels RJ: Tissue kallikrein stimulates Ca<sup>2+</sup> reabsorption via PKC-dependent plasma membrane accumulation of TRPV5. *EMBO J* 25: 4707–4716, 2006
- van der Wal J, Habets R, Varnai P, Balla T, Jalink K: Monitoring agonist-induced phospholipase C activation in live cells by fluorescence resonance energy transfer. *J Biol Chem* 276: 15337–15344, 2001
- Ponsioen B, Zhao J, Riedl J, Zwartkruis F, van der Krogt G, Zaccolo M, Moolenaar WH, Bos JL, Jalink K: Detecting cAMP-induced Epac activation by fluorescence resonance energy transfer: Epac as a novel cAMP indicator. *EMBO Rep* 5: 1176–1180, 2004
- Varnai P, Balla T: Visualization of phosphoinositides that bind pleckstrin homology domains: Calcium- and agonist-induced dynamic changes and relationship to myo-[<sup>3</sup>H]inositol-labeled phosphoinositide pools. *J Cell Biol* 143: 501–510, 1998
- Chijiwa T, Mishima A, Hagiwara M, Sano M, Hayashi K, Inoue T, Naito K, Toshioka T, Hidaka H: Inhibition of forskolin-induced neurite outgrowth and protein phosphorylation by a newly synthesized selective inhibitor of cyclic AMP-dependent protein kinase, N-[2-(p-bromocinnamylamino)ethyl]-5-isoquinolinesulfonamide (H-89), of PC12D pheochromocytoma cells. *J Biol Chem* 265: 5267–5272, 1990
- Bianco SD, Peng JB, Takanaga H, Suzuki Y, Crescenzi A, Kos CH, Zhuang L, Freeman MR, Gouveia CH, Wu J, Luo H, Mauro T, Brown EM, Hediger MA: Marked disturbance of calcium homeostasis in mice with targeted disruption of the Trpv6 calcium channel gene. *J Bone Miner Res* 22: 274–285, 2007
- Naraghi M: T-jump study of calcium binding kinetics of calcium chelators. *Cell Calcium* 22: 255–268, 1997
- Leathers VL, Linse S, Forsen S, Norman AW: Calbindin-D28K, a 1  $\alpha$ ,25-dihydroxyvitamin D<sub>3</sub>-induced calcium-binding protein, binds five or six Ca<sup>2+</sup> ions with high affinity. *J Biol Chem* 265: 9838–9841, 1990
- Lambers TT, Mahieu F, Oancea E, Hoofd L, de Lange F, Mensenkamp AR, Voets T, Nilius B, Clapham DE, Hoenderop JG, Bindels RJ: Calbindin-D28K dynamically controls TRPV5-mediated Ca<sup>2+</sup> transport. *EMBO J* 25: 2978–2988, 2006
- Nilius B, Vennekens R, Prenen J, Hoenderop JG, Bindels RJ, Droogmans G: Whole-cell and single channel monovalent cation currents through the novel rabbit epithelial Ca<sup>2+</sup> channel ECaC. *J Physiol* 527: 239–248, 2000
- Hoenderop JG, Willems PH, Bindels RJ: Toward a comprehensive molecular model of active calcium reabsorption. *Am J Physiol Renal Physiol* 278: F352–F360, 2000
- Kiebzak GM, Yusufi AN, Kusano E, Braun-Werness J, Dousa TP: ATP



- and cAMP system in the *in vitro* response of microdissected cortical tubules to PTH. *Am J Physiol* 248: F152–F159, 1985
35. Griffiths NM, Brick-Ghannam C, Siaume-Perez S, Chabardes D: Effect of prostaglandin E2 on agonist-stimulated cAMP accumulation in the distal convoluted tubule isolated from the rabbit kidney. *Pflugers Arch* 422: 577–584, 1993
  36. Wrenn RW, Biddulph DM: Parathyroid hormone-induced calcium efflux from isolated renal cortical tubules: Evidence for cyclic AMP mediation. *Mol Cell Endocrinol* 15: 29–40, 1979
  37. Shareghi GR, Stoner LC: Calcium transport across segments of the rabbit distal nephron *in vitro*. *Am J Physiol* 235: F367–F375, 1978
  38. Hoenderop JG, van der Kemp AW, Hartog A, van de Graaf SF, van Os CH, Willems PH, Bindels RJ: Molecular identification of the apical Ca<sup>2+</sup> channel in 1, 25-dihydroxyvitamin D<sub>3</sub>-responsive epithelia. *J Biol Chem* 274: 8375–8378, 1999
  39. Kilhoffer MC, Haiech J, Demaille JG: Ion binding to calmodulin: A comparison with other intracellular calcium-binding proteins. *Mol Cell Biochem* 51: 33–54, 1983
  40. Feller MB, Delaney KR, Tank DW: Presynaptic calcium dynamics at the frog retinotectal synapse. *J Neurophysiol* 76: 381–400, 1996
  41. Sooy K, Kohut J, Christakos S: The role of calbindin and 1,25-dihydroxyvitamin D<sub>3</sub> in the kidney. *Curr Opin Nephrol Hypertens* 9: 341–347, 2000
  42. Perez AV, Picotto G, Carpentieri AR, Rivoira MA, Peralta Lopez ME, Tolosa de Talamoni NG: Minireview on regulation of intestinal calcium absorption: Emphasis on molecular mechanisms of transcellular pathway. *Digestion* 77: 22–34, 2008
  43. Cha SK, Jabbar W, Xie J, Huang CL: Regulation of TRPV5 single-channel activity by intracellular pH. *J Membr Biol* 220: 79–85, 2007
  44. den Dekker E, Schoeber J, Topala CN, van de Graaf SF, Hoenderop JG, Bindels RJ: Characterization of a Madin-Darby canine kidney cell line stably expressing TRPV5. *Pflugers Arch* 450: 236–244, 2005
  45. Hoenderop JG, Nilius B, Bindels RJ: Molecular mechanism of active Ca<sup>2+</sup> reabsorption in the distal nephron. *Annu Rev Physiol* 64: 529–549, 2002
  46. Friedman PA, Coutermarsh BA, Kennedy SM, Gesek FA: Parathyroid hormone stimulation of calcium transport is mediated by dual signaling mechanisms involving protein kinase A and protein kinase C. *Endocrinology* 137: 13–20, 1996
  47. Nilius B, Prenen J, Hoenderop JG, Vennekens R, Hoefs S, Weidema AF, Droogmans G, Bindels RJ: Fast and slow inactivation kinetics of the Ca<sup>2+</sup> channels ECaC1 and ECaC2 (TRPV5 and TRPV6). Role of the intracellular loop located between transmembrane segments 2 and 3. *J Biol Chem* 277: 30852–30858, 2002
  48. Lambers TT, Weidema AF, Nilius B, Hoenderop JG, Bindels RJ: Regulation of the mouse epithelial Ca<sup>2+</sup> channel TRPV6 by the Ca<sup>2+</sup>-sensor calmodulin. *J Biol Chem* 279: 28855–28861, 2004
  49. van de Graaf SF, Hoenderop JG, Gkika D, Lamers D, Prenen J, Rescher U, Gerke V, Staub O, Nilius B, Bindels RJ: Functional expression of the epithelial Ca<sup>2+</sup> channels (TRPV5 and TRPV6) requires association of the S100A10-annexin 2 complex. *EMBO J* 22: 1478–1487, 2003
  50. Ward CA, Giles WR: Ionic mechanism of the effects of hydrogen peroxide in rat ventricular myocytes. *J Physiol* 500: 631–642, 1997

---

Supplemental information for this article is available online at <http://www.jasn.org/>.